Proceedings of the
International Conference on Mechanical Engineering 2011
(ICME2011) 18-20 December 2011, Dhaka, Bangladesh

ICME 11-AM-029

EFFECT OF STRAIN HARDENING ON UNLOADING OF A DEFORMABLE SPHERICAL CONTACT UNDER STICK CONTACT CONDITION – A FINITE ELEMENT STUDY

Biplab Chatterjee and Prasanta Sahoo

Department of Mechanical Engineering, Jadavpur University, Kolkata, India

ABSTRACT

The present study explores the effect of strain hardening on unloading of an elastic-plastic sphere against a rigid flat under full stick contact condition. Commercial finite element software ANSYS is used to analyze the contact parameters like load, area, residual interference with different tangent modulus. Tangent modulus indicates the extent of strain hardening and is varied with hardening parameter. Most of the practical materials are within the range of hardening parameters that is covered in this work. Both the kinematic and isotropic hardening rules are considered in a non-adhesive infinite friction contact condition. The simulations of finite element analysis are compared with perfect slip contact condition and other available literature for full stick contact condition. It is observed that the contact conditions have negligible effect on contact parameters. It is found that the contact parameters during loading unloading are not in uniform nature within the range of hardening parameters used in this study.

Keywords: Elastic-Plastic Contact, Strain Hardening, Hardening Rule.

1. INTRODUCTION

Loading unloading is inevitable in all the engineering applications to transmit force, motion and power etc. It is found in metal forming, machining or other manufacturing processes. When studied carefully on a very fine scale, all solid surfaces are found to be rough with asperities. For the simplicity of calculation, asperities are assumed of spherical shape. The study of elastic plastic contact of a deformable sphere with a rigid flat gives an intuition about the happenings when two rough surfaces are in contact. It is possible to predict the elastic response of solids under frictionless contact condition using Hertz [1] theory. The stress is proportional to the strain within the elastic limit and the deformation is reversible. If the stress exceeds the critical value, the material is plastically deformed and there is no longer a linear relationship between the stress and strain as there is for elastic deformation. There is permanent change in shape on unloading. The behaviors of materials that have been stressed beyond the elastic region are usually described with bilinear hardening using tangent modulus. Kogut and Etsion[2] (KE Model) provided an accurate result of elastio-plastic contact of a hemisphere and a rigid flat under frictionless contact condition during loading. They investigated the effect of tangent modulus by varying it up to 0.1E. KE found with tangent modulus of 0.1E, the difference of resulting contact parameters with that of elastic perfectly plastic material was less than 20%. Etsion et al. [3] provided a model of universal nature, which was independent of the physical and geometrical properties of the sphere during unloading of an elastic-plastic loaded spherical contact with a rigid flat under perfect slip contact condition using commercial finite element software ANSYS. They choose 2% isotropic linear hardening and observed a marginal variation of results with that of elastic perfectly plastic material. Kadin et al. [4] studied the multiple loading unloading of a deformable sphere against a rigid flat under frictionless contact condition. They observed slight additional hardening during the first unloading compared to the first loading. This hardening causes secondary plastic flow. They inferred that the incipient interference to cause secondary plastic flow increases with the increase in strain hardening. Shankar and Mayuram [5] studied the elastic-plastic transition behavior in a hemisphere in contact with a rigid flat under frictionless contact condition accounting for the effect of realistic material behavior in terms of the varying yield strengths and the isotropic strain hardening. They used three tangent modulus, 0.025E, 0.05E and 0.1E and inferred that with the increase in tangent modulus, the transition from elastic-plastic to fully plastic state occurs in less dimensionless interference ratio. Sahoo et al. [6] introduced hardening parameter, which caters more practical approach to study the effect of strain hardening on interfacial parameters of deformable sphere with a rigid flat under frictionless contact condition during loading. They used hardening parameter (H) ranging from 0 to 0.5. Most of the materials fall in the range and enabled them to study the effect of strain hardening with tangent modulus as high as 0.33E. Sahoo et al. inferred that with the increase in strain hardening the resistance to deformation of a material is increased and the material becomes capable of carrying higher amount of load in a smaller contact area. Chatterjee and Sahoo [7] analyzed the effect of strain hardening during unloading of an elastic

plastic loaded sphere against a rigid flat under frictionless contact condition using finite element software. They observed that higher tangent modulus (strain hardening) results lower residual interference when unloaded from a particular dimensionless interference; which in turn offer less resistance to full recovery of the original shape. Several authors replaced the work of perfect slip contact condition by full stick contact condition. Brizmer et al. [8] first analyzed the effect of full stick condition on the elasticity terminus of a spherical contact using finite element software ANSYS. They found the increasing differences with decreasing Poisson's ratio compared to the perfect slip contact condition. Brizmer et al. [9] extended their study for the loading of an elastic plastic spherical contact both under full stick and perfect slip contact condition with 2% isotropic linear hardening and found the interfacial parameters are insensitive to the contact condition and material properties of the deformable sphere. However they concluded that the contact load, average contact pressure is slightly affected by Poisson's ratio for full stick contact condition. Zait et al. [10] performed the unloading of an elastic-plastic spherical contact under full stick contact condition with 2% isotropic linear hardening. They found a substantial variation in load area curve during unloading under full stick contact condition compared to that of under perfect slip contact condition.

The effect of strain hardening can be studied by relating the size and shape of the yield surface to plastic strain in some appropriate way [11]. Most of the elastic plastic contact models available in the literature are based either on linear isotropic hardening or with elastic perfectly plastic materials. Some of finite element models have also been proposed to simulate multiple, cyclic loading unloading using bilinear kinematic hardening. Zait et al. [12] used both isotropic and kinematic hardening during the study of multiple normal loading unloading cycles of a spherical contact under stick contact condition. They observed that the cyclic loading under stick contact condition converged into elastic shake down with both the isotropic and kinematic hardening model. Zait et al. cited the reason behind the similar results with both the hardening model as the use of small amplitudes during multiple loading unloading. Kadin et al. [13] adopted 2% bilinear kinematic hardening while analyzing the loading unloading of an elastic plastic adhesive spherical micro contact. They reported that the kinematic hardening produced more realistic plastic shakedown compared to elastic shake down with isotropic hardening. Ovcharenko et al. [14] published the experimental results of real contact area between a sphere and a flat during loading, unloading, and cyclic loading unloading in the elastic plastic regime. Their experimental results of multiple loading unloading had a tendency to shakedown. The results indicated an increase in contact area with increasing number of loading cycles. Song and Komvopoulos [15] studied the adhesive contact of a rigid sphere with elastic perfectly plastic half space. They concluded that the high Tabor parameter and low plasticity parameter resulted in elastic shakedown whereas low Tabor parameter and high plasticity parameter resulted in plastic shakedown. Kadin et al. [16] compared the results with isotropic and kinematic hardening while performing cyclic loading of an elastic plastic adhesive spherical micro contact. They reported that for single loading cycle, different hardening model yield similar results but kinematic hardening model is necessary in case of unloading and cyclic loading. Zolotarevskiy et al. [17] found the tangential displacement at the completion of the first loading unloading are larger in case of the isotropic hardening compared to that in kinematic hardening.

It is clear from the foregoing discussion, different hardening model may provide results with distinct variation even for single loading unloading in case of large deformation. But so far our knowledge, single loading unloading stick contact analysis for large deformation with isotropic and kinematic hardening for various strain hardening is still missing in literature. The present work is therefore an attempt to quantify the effect of strain hardening on residual interference, load- real contact area behavior during unloading under full stick contact condition with isotropic and kinematic hardening.

2. THEORETICAL BACKGROUND

The effect of strain hardening is studied using spherical contact of a deformable sphere with a rigid flat under full stick contact condition. Figure 1 is a schematic diagram of a deformable hemisphere with a rigid flat.

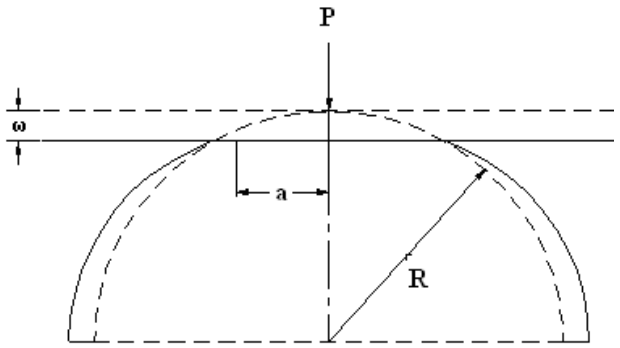

Fig 1. A schematic diagram of a deformable sphere pressed by a rigid flat.

The dashed line presents the original contour of the sphere, having a radius of R, and the rigid flat before the deformation. The solid line shows the loading phase with the interference of ω, corresponding to the contact radius (a) and the contact load (P).

The solution consists of two stages. In the first one we have applied a displacement on the rigid flat by a dimensionless interference $\omega^* = \omega / \omega_c$. During this stage the interference ω is gradually increased up to a desired maximum value, ω_{max}, and the contact load, the real contact area reach their maximum value P_{max}, A_{max} respectively. The second stage consists of the unloading process, where the interference, ω, is gradually reduced. At the end of the unloading, under zero contact load and contact area, the sphere has a residual interference (ω_{res}). Therefore the original un-deformed spherical geometry is not fully recovered. The original profile, the deformed shape after loading phase and the sphere profile at the end of unloading are represented in figure 2. Stick contact condition is applied at the interface of the deformed sphere

and the rigid flat. The stick contact condition prevents the contact point of the deformed sphere with the rigid flat from the relative displacement in the radial direction but it allows the axial detachment of the sphere surface from the rigid flat during unloading.

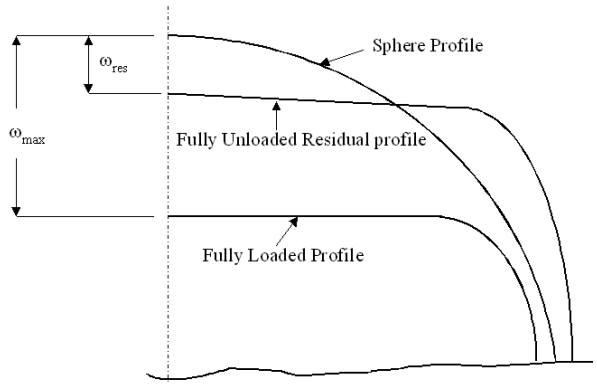

Fig 2. Three different profiles of the sphere.

Tangent modulus (E_t) is the slope of the stress-strain curve. Below the proportional limit the tangent modulus is the same as the Young's modulus. Above the proportional limit the tangent modulus varies with the strain. The tangent modulus is useful in describing the behavior of materials that have been stressed beyond the elastic region. All the materials follow the multi-linear behavior with some tangent modulus. This multi-linear behavior can be assumed as bilinear behavior for analysis purpose in elastic-plastic cases. In this analysis a bilinear material property is provided for the deformable hemisphere. To study the strain hardening effect we have taken different values of tangent modulus (E_t). The Tangent Modulus (E_t) is varied according to a parameter, which is known as Hardening parameter and defined as, $H = \frac{E_t}{E - E_t}$. The value of H is taken in the range $0 \le H \le 0.5$. The value of H equals to zero indicates elastic perfectly plastic material behavior, which is an idealized material behavior. The hardening parameters used for this analysis and their corresponding values are shown in Table 1. The wide range of values of tangent modulus is taken to make a fair idea of the effect of strain hardening in single asperity under full stick contact condition with the other material properties are taken as constant.

The type of strain hardening depends on the size and shape of the yield surface to plastic strain. We have studied here with both isotropic and kinematic bilinear hardening. The results are compared with the findings under perfect slip contact condition and other results available under full stick contact condition. figure 3 presents the difference between isotropic and kinematic bilinear hardening by describing the development of yield surface with progressive yielding. In isotropic or work hardening the yield surface is uniformly spread out from the center (figure 3(a)) while in kinematic hardening the yield surface translates in stress space with constant in size (figure 3(b)).

Table 1: Different H and E_t values used for the study of strain hardening effect

H	E_t in %E	E_t (GPa)
0	0.0	0.0
0.1	9.0	6.3
0.2	16.7	11.7
0.3	23.0	16.1
0.4	28.6	20.0
0.5	33.0	23.1

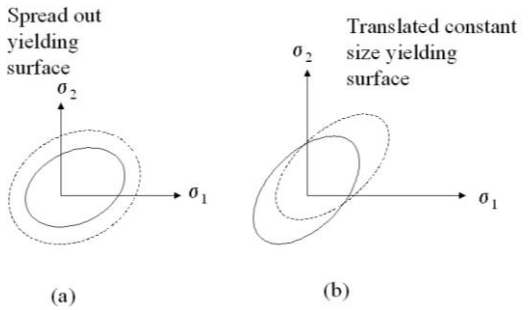

Fig 3 (a). Isotropic and (b) Kinematic hardening models for two-dimensional stress field.

Brizzer et al [8] provided the empirical relations for critical interference and corresponding values for critical loads and critical contact area for perfect slip and full stick contact conditions. For full stick contact condition, the contact parameters are normalized using the Brimer et al [8] expression for critical interference (ω_c), critical load (P_c) and critical contact area (A_c) for full stick contact condition to form dimensionless parameters as follows.

$$\omega_c = (C_\nu \frac{\pi(1-\nu^2)}{2}(\frac{y}{E}))^2 R(6.82\nu - 7.83(\nu^2 + 0.0586)) \quad (1)$$

$$P_c = \frac{\pi^3 Y}{6} C_\nu^3 (R(1-\nu^2)(\frac{Y}{E}))^2 (8.88\nu - 10.13(\nu^2 + 0.089)) \quad (2)$$

$$A_c = \pi \omega_c R \quad (3)$$

Where $C_\nu = 1.234 + 1.256\nu$. The parameters Y, E, and ν are the virgin yield stress, the Young modulus, and Poisson's ratio of the sphere material, respectively and R is the radius of the sphere. The sphere size is used for this analysis is R = 1 μm. The material properties used here are Young's Modulus (E) = 70 GPa, Poisson's Ratio (ν) = 0.3 and Yield stress (σ_y) = 100 MPa. For full stick contact condition, infinite friction condition is adopted.

3. FINITE ELEMENT MODEL

An axisymmetric 2-D model is used to reduce the time of computation as well as to simulate accurate results. The present study utilizes the commercial FE software ANSYS 11.0. The sphere is modeled by a quarter of a circle, due to its axisymmetry. A line models the rigid flat. Six node triangular axisymmetric elements (plane183) are used in

the present model. The model refines the element mesh near the region of contact to allow the sphere's curvature to be captured and accurately simulated during deformation. The mesh consists of maximum 18653 six node triangular axisymmetric elements (plane183) comprising 37731 nodes. The resulting ANSYS mesh is presented in figure 4.

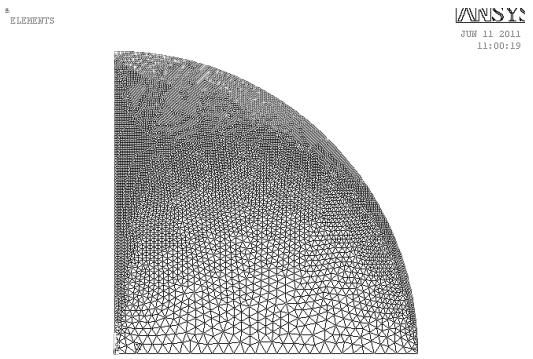

Fig 4. Finite element mesh of sphere in ANSYS

The nodes on the axis of symmetry are fixed in radial direction. Likewise the nodes on the bottom of the hemisphere are fixed in both axial and radial direction. Both the bilinear kinematic (BKIN) and isotropic hardening (BISO) options in the ANSYS program are chosen to account the elastic-plastic material response for the single asperity model with two different hardening rule The rate independent plasticity algorithm incorporates the von Mises criterion. The mesh density is iteratively increased until the contact force and contact area differed by less than 1%between the iterations. In addition to mesh convergence, the model also compares well with the Hertz elastic solution at interferences below the critical interference. This work uses Lagrangian multiplier method. The tolerance of current work is set to 1% of the element width. Computations took about 5 minutes for small interferences and 30-40 minutes for large interferences in a 1.6GHz. PC.

4. RESULTS AND DISCUSSION

Dimensionless contact loads (P^*) are plotted as a function of dimensionless interference (ω^*) during loading unloading under full stick contact condition with kinematic hardening in figure 5(a), 5(b) and with isotropic hardening in figure 6(a), 6(b). The dimensionless contact loads are increasing with the increase in tangent modulus during loading of an elastic plastic spherical contact under full stick contact condition and this dimensionless contact load is higher for isotropic hardening model than that of kinematic hardening model at larger interference. The variation is not more than 5% for higher tangent modulus at the dimensionless interference as large as 200 times of critical interference though for elastic perfectly plastic material the dimensionless contact load for both the hardening model is exactly same even if for larger interference.

The numerical results of the unloading process initiated from two representative ω_{max}^* values of 200 and 150. When the unloading process is completed, the contact load fall to zero at certain dimensionless interference ω^*_{res} (ω_{res}/ω_c). ω^*_{res} increases with the decrease of strain hardening (tangent modulus.) irrespective of maximum loading ω^*_{max}; from which unloading is started. It is found from the figures that the residual interferences as well as residual strain ($\omega_{res}/\omega_{max}$) with kinematic hardenings are less compared to the corresponding residual interferences /residual strain with isotropic hardening when unloaded from a specific maximum dimensionless interference. The material with less residual strain releases more energy compared with the material, which keep more residual strain after unloading. These results are in good agreement with the observation of Zolotarevskiy et al. [17] who observed that the tangential displacement after the completion of the first unloading is larger in case of the isotropic hardening compared to that in kinematic hardening. The present results have been compared with the findings under perfect slip contact condition using isotropic hardening of Chatterjee and Sahoo [7]. It is found, the residual interferences for full stick contact condition are nearly same with the corresponding residual interferences of perfect slip contact condition.

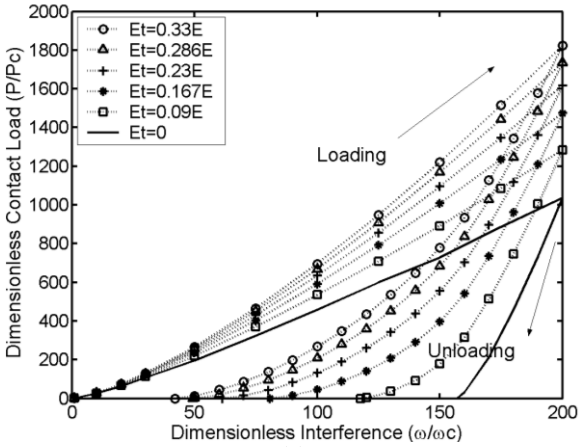

(a)

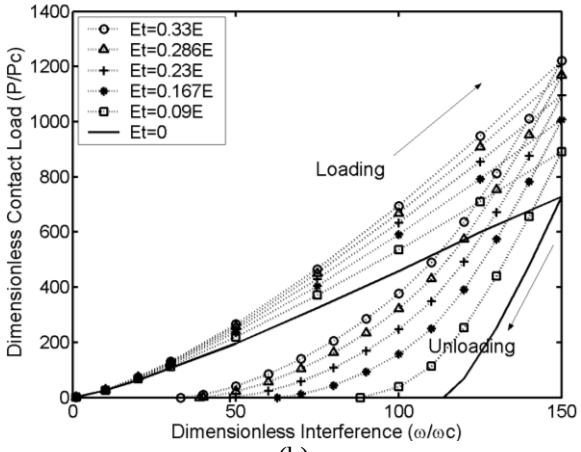

(b)

Fig 5. Dimensionless contact load at full stick contact condition with kinematic hardening; Unloaded from dimensionless interference of (a) ω_{max} =200 (b) ω_{max}= 150

Finite element simulation indicates that the residual interference with kinematic hardening is always less than the corresponding value of isotropic hardening when unloaded from a specific dimensionless interference. As

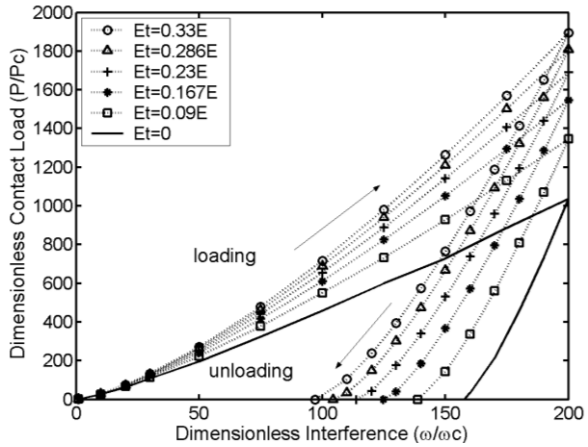

(a)

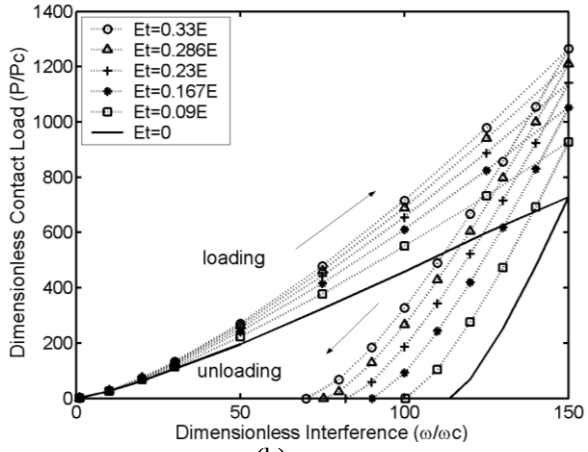

(b)

Fig 6. Dimensionless contact load at full stick contact condition with isotropic hardening; Unloaded from dimensionless interference of (a) ω_{max} =200 (b) ω_{max}= 150.

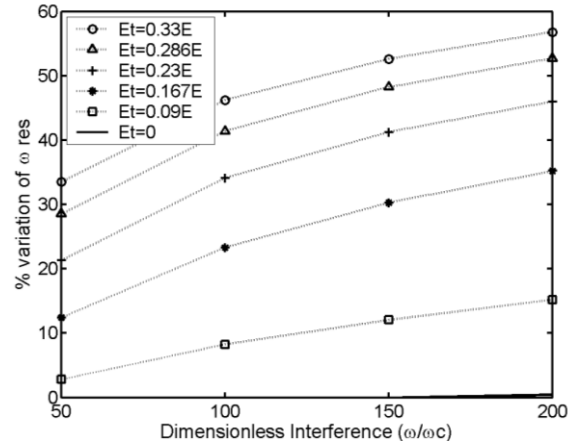

Fig 7. Percentage variations of residual interferences with kinematic hardening in comparison with the corresponding value using isotropic hardening.

can be seen from figure 7,the variation increases with the increase in strain hardening (higher tangent modulus) and with the increase in dimensionless interference from where unloading initiates for the same tangent modulus. For the large hardening paramete $H = 0.5$ (Et=0.33E), the residual interferences are 33.5% to 56.8% less compared with the residual interference using isotropic hardening.

For the hardening parameter $H = 0.1$ (Et=0.09E), the variation ranges from 2.8% to 15.2% whereas in case of elastic perfectly plastic material, both the hardening rule yields almost identical results. The maximum variation is 0.41% and it is found when the unloading starts from ω_{max}=200 for elastic perfectly plastic material.

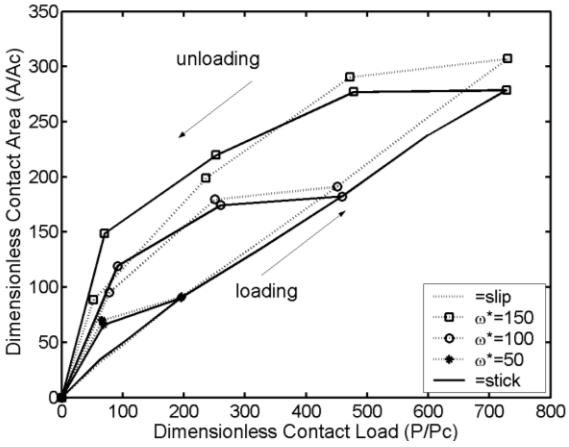

Fig 8. A^* Vs P^* for two different contact condition unloaded from different maximum dimensionless interference for elastic perfectly plastic material

Figure 8 shows the dimensionless contact area Vs dimensionless contact load for loading and unloading under both the perfect slip and full stick contact condition for elastic perfectly plastic sphere (Et=0) against a rigid flat. The plot has been made for unloading from different maximum dimensionless interferences. It is clear from the figure, at the beginning of unloading the dimensionless contact area for perfect slip contact condition is larger than that of the dimensionless contact area for full stick contact condition when unloaded from dimensionless interference of ω*=150.However from about ω*= 135, onwards the dimensionless contact area for perfect slip contact condition is less than the dimensionless contact area for full stick contact condition during unloading. When unloaded from ω*=100, the same trend is observed, that is at the beginning of unloading the dimensionless contact area for perfect slip contact condition is larger than the dimensionless contact area for full stick contact condition and at the tail end of unloading the contact area for perfect slip contact condition is less than that of full stick condition. However when unloaded from ω*=50, the dimensionless contact areas for both the contact condition during unloading are nearly identical. These results may seemingly counterintuitive with the findings of Zait et al. [10], (Figure 9). Zait et al. [10] took identical loading curves for both the contact conditions with the average of wide range of E/Y ratio (E/Y=500-1000), Poisson's ratio as 0.32 and linear hardening of 2%. But the fact for elastic perfectly plastic materials with a specific E/Y ratio is that, though the contact condition has little effect on the dimensionless contact load, the contact area behaves differently. For perfect slip contact condition the compressible sphere material tends to displace inward during loading up to ω*=22, above which, the last contact point displaces in outward direction (Jackson and Green [18]). The outward displacement depends on E/Y ratio. The radial displacement is held back by the stick

contact condition imposed by rigid flat. From the finite element analysis it reveals, while the dimensionless contact area for perfect slip contact condition is smaller than the corresponding value for full stick contact condition at low dimensionless interference but at higher interference the dimensionless contact area for perfect slip contact condition is higher than the corresponding value for full stick contact condition during loading. Zait et al. [10] also explained these phenomena during the investigation of shear stress (Figure 5).

5. CONCLUSIONS

The load interference behavior during loading unloading under full stick contact condition is nearly identical for both the contact condition with a specific strain hardening when other material properties are constant. It was observed that higher tangent modulus (strain hardening) results lower residual interference when unloaded from a particular dimensionless interference; which in turn offers less resistance to full recovery of the original shape irrespective of contact condition and hardening rule. The residual interferences with kinematic hardening are always less in comparison with the corresponding value using isotropic hardening for bilinear hardened material. The kinematic hardened material dissipates more energy during unloading than isotropic hardened material. The variation of the dissipated energy increases with the increase in strain hardening (higher tangent modulus) and the level of loading. However the response of hardening rule is insignificant in case of elastic perfectly plastic materials. The dimensionless contact area under full stick contact condition is larger than that of under perfect slip contact condition during unloading for higher strain hardening.

6. REFERENCES

1. Hertz, H., 1882, "Über die Berührung fester elastischer Köper", J. Reine and Angewandte Mathematik, 92:156-171.
2. Kogut, L and Etsion, I., 2002, " Elastic-plastic contact analysis of a sphere and a rigid flat", ASME J. Appl. Mech , 69: 657-662.
3. Etsion, I., Kligerman, Y. and Kadin, Y., 2005, "Unloading of an elastic-plastic loaded spherical contact", Int. J. Solid Struct., 42: 3716-3729.
4. Kadin, Y., Kligerman, Y. and Etsion, I., 2007,"Multiple loading-unloading of an elastic-plastic spherical contact", Int. J. Solids Struct.,43: 7119-7127.
5. Shankar, S. and Mayuram, M. M., 2008, "Effect of strain hardening in elastic-plastic transition behavior in a hemisphere in contact with a rigid flat", International Journal of solids and structure, 45:3009-3020.
6. Sahoo, P., Chatterjee, B. and Adhikary, D., 2010, "Finite element based Elastic-plastic contact behavior of a sphere against a rigid flat- Effect of Strain Hardening", Int. J. Engg. and Tech., 2: 1-6.
7. Chatterjee, B. and Sahoo, P., 2010, "Effect of strain hardening on unloading of a deformable sphere loaded against a rigid flat- A finite element study", Int. J. Engg. and Tech., 2(4): 225-233.
8. Brizmer, V., Kligerman, Y. and Etsion, I., 2006, "The effect of contact conditions and material properties on the elasticity terminus of a spherical contact", Int. J. Solid Struct., 43: 5736-5749.
9. Brizmer, V., Kligerman, Y. and Etsion, I., 2006, "The effect of contact conditions and material properties on elastic-plastic spherical contact", J. Mech. Mater. and Struct., 1(5): 865-879.
10. Zait, Y., Kligerman, Y. and Etsion, I., 2010,"Unloading of an elastic-plastic spherical contact under stick contact condition", Int. J. Solid Struct., 47:990-997.
11. Bower, F. A., 2008, *Applied Mechanics of solids*, CRC press, NW, USA.
12. Zait, Y., Zolotarevsky, V., Kligerman, Y. and Etsion, I., 2010, "Multiple normal loading cycles of a spherical contact under stick contact condition", Journal of Tribology, 132: 041401-1-7.
13. Kadin, Y., Kligerman, Y. and Etsion, I., 2008,"Loading-unloading of an elastic-plastic adhesive spherical micro contact", J. Colloid and Interface Sci., 321: 242-250.
14. Ovcharenko, A., Halperin, G., Verberne, G. and Etsion, I., 2007, "In situ investigation of the contact area in elastic-plastic spherical contact during loading-unloading", Tribol.Lett., 25:153-160.
15. Song, Z. and Komvopoulos, K., 2011, "Adhesion-induced instability in elastic and elastic-plastic contacts during single and repetitive normal loading", J. Mech. and Phys. solids, 59: 884-897.
16. Kadin, Y., Kligerman, Y. and Etsion, I., 2008, "Cyclic loading of an elastic-plastic adhesive spherical micro contact", J. Appl. Phys., 104: 073522-1-8.
17. Zolotarevsky, V., Kligerman, Y. and Etsion, I., 2011,"Elastic-plastic spherical contact under cyclic tangential loading in pre-sliding", Wear, 270: 888-894.
18. Jackson, R. L. and Green, I., 2005, "A finite element study of elasto-plastic hemispherical contact against a rigid flat", ASME J. Tribol., 127:343-354.

7. NOMENCLATURE

Symbol	Meaning	Unit
P	Contact load	(N)
R	Radius of the sphere	(μm)
p	Pressure	(GPa)
ω	Interference	(μm)
A	Contact area	(μm^2)
E	Modulus of Elasticity	(GPa)
Y	Yield strength of sphere	(GPa)
ν	Poison's ratio	
E_t	Tangent modulus of the sphere	(GPa)
P^*	Dimensionless contact load, P/P_c in stick contact	
A^*	Dimensionless contact area, A/A_c in stick contact	
ω^*	Dimensionless interference,ω/ω_c in stick contact	

8. MAILING ADDRESS

Biplab Chatterjee
Department of Mechanical Engineering,
Jadavpur University, Kolkata 700032, India
Fax: +91 33 2414 6890
E-mail: psjume@gmail.com,